Journal of Engineering Science and Technology
Vol. 13, No. 11 (2018) 3764 - 3780

ANALYSIS OF DISTRIBUTED DEFECT ON OUTER RING OF BALL BEARING UNDER RADIAL LOAD: A THEORETICAL AND EXPERIMENTAL APPROACH

SHAM S. KULKARNI*, ANAND K. BEWOOR

[1]Sinhgad College of Engineering Vadgaon, Pune (MH)-411 041, India
[2]MKSSS's College of Engineering for Women, Pune (MH)-411052, India
*Corresponding Author: shamk43@gmail.com

Abstract

The paper reports development of a theoretical model to study vibration characteristics of the ball bearing. The Lagrangian method is adopted to analyse vibrations generated due to circumferential motions of the ball as well as its contact with an inner and outer ring. The contact between the ball and bearing rings are assumed to be of nonlinear spring whose stiffness is computed using Hertz theory. The Runge Kutta method is implemented to solve nonlinear equations of motion. The effect of extended outer raceway defect size and speed on the vibration characteristics of the ball bearing is analysed. The frequency domain transformation indicates that vibration characteristic of ball bearing varies as a result of nonlinear load deflection relation during the interaction of ball and raceway defect. The analysis implied that defect size and speed of the ball bearing are influencing parameters affecting the dynamic response of the bearing.

Keywords: Ball bearing, Distributed defect, Lagrangian method, Hertz theory, Runge-Kutta method, Vibration.

1. Introduction

Bearings plays a crucial role in the operation of rotating machinery and extensively used in a variety of industries such as sugar industry, construction, mining, paper mills, railway and renewable energy. Dynamic performance of rotating machine is greatly influenced by bearing vibrations [1]. The reliability of the bearing is most prominent in overall machine performance. In industrial areas, these bearings are deliberated as critical mechanical components and a defect in such bearings, if not detected in time, causes breakdown and may even cause disastrous failure of machinery. In most of the sugar industry applications, the deep groove ball bearings used in cranes for carrying sugar bags and canes are subjected to fatigue spalling. Moreover, micro-scale fatigue cracks are initiated below highly stressed region of bearing under continuous loading. In such area of maximum stresses, microstructural discontinuities generate a micro-plastic deformation [2].The cyclic loading during bearing operation, existing fatigue crack continues to spread along the periphery of the rolling surface. The rolling element bearings damage leads to increase the machinery breakdown consequently costing the significant economical losses. The defects in bearings are mainly classified into three categories-localized, distributed and extended defects. Localized defects include a crack, pits and spalls generated on various elements of bearing on account of fatigue while distributed defects consist of waviness and off size ball is created due to the manufacturing error and working conditions [3]. Whereas, an extended defect can be characterized as a defect namely larger than a local fault but smaller than a waviness [19]. Numerous techniques have been adopted [4, 5] such as high-frequency resonance technique, localized current method, sound measurement technique and acoustic emission technique for bearing fault detection. Vibration-based detection techniques for monitoring the health of bearings have been widely used in both time and frequency domain.

In the analysis of local defects, the contribution is made in the development of periodic models, Quasiperiodic modes, and multibody dynamics models. The primary objective of these reviewed models was to analyse vibration characteristics of bearing due to the interaction of rolling element at entrance and exit of bearing defect. It has been observed that impact time difference between vibration signal at entry and exit edge of the defect are exactly correlating with the size of defects. The developments of local defect models have been initiated by McFadden and Smith [6] and Choudhary [7]. They predicted vibration frequencies and amplitude of significant frequencies of rolling element bearing due to local defects under radial and axial load. It has been concluded that the position-dependent characteristic defect frequencies are used to detect the existence of a defect and also diagnose its location. Moreover, many theoretical models have also been formulated by Newton's equation of motions [8, 9]. In addition to this, the effect of radial clearance and unbalance excitation of the system have also been analysed in the model development of ball bearing [10].

In case of distributed defect analysis, the analytical model has been proposed [11] to analyse characteristics of vibrations of the ball bearing. The prediction of spectral components on account of distributed defects in the bearing is made and compared with simulated results. It has been concluded that level of vibration is dependent on the combined order of waviness of both inner and outer race of bearing. Moreover, a discrete spectrum of a specific frequency component for each order of waviness [12] is observed during the analysis of bearing with distributed

fault. Recently, some of the *researchers* [13, 14] have carried out analysis on the inner race waviness and reported that with an increase in a number of balls results in the reduction of ball pass frequency, however amplitude of vibration increases as waviness on inner ring increases. Further, a new stochastic model was also introduced [15] for ball bearing with roughness on its races and concluded that stochastic excitation increases with increase in defect size and roughness of contacting surfaces. In contrast to localized and distributed defects, extended defects have received less attention. From existing literature, only two publications had discussed the vibration modeling of rolling element bearing with an extended defect [16, 17]. They have predicted vibration characteristic of bearing with extended raceway defects.

The impulsive forces can be generated during continuous and repetitive movement of rolling element over the local defect. This repeated operation during re-stressing of the rolling elements wears the trailing edge of the spall causing it to gradually propagate in size and results in the generation of extended defects. The present paper develops a mathematical model for extended nature of distributed fault based on two degrees of freedom. The theoretical model based on Lagrangian approach is developed to study the effect of speed and defect size on the dynamic response of bearing. Outer ring defect analysis has been modelled as a sinusoidal wave. Runge Kutta method is adopted to solve nonlinear equations. The contact forces due to outer race defect of bearing is analysed using hertzian contact theory. A dynamic model is validated by conducting experiments. The response of theoretical model and results of the experimental study have been compared to a single defect on the outer ring of bearing. The results of the theoretical model show good agreement with experimental vibration response.

2. Defect Frequencies

The defect present in the bearing element tends to increase vibration energy at defect frequency. These defect frequencies mainly depend upon shaft rotation and bearing dimensions. The characteristic defect frequencies [18] are computed as follows:

Outer ring defect frequency (BPFO)

$$f_o = \frac{(n_b \times \mathrm{f}_s)}{2}[1 - \frac{d_b}{D_p}\cos\alpha\,] \tag{1}$$

Inner ring defect frequency (BPFI)

$$f_i = \frac{(n_b \times \mathrm{f}_s)}{2}[1 + \frac{d_b}{D_p}\cos\alpha\,] \tag{2}$$

3. Ball Bearing Model

A model has been developed to estimate vibration characteristics of the ball bearing. Figure 1 depicts the schematic diagram of ball bearings, which shows the various elements of bearing. During modeling, it is assumed that the outer ring of the bearing is rigidly fixed. Hertzian contact theory is used to determine elastic deformation between ball and rings, considering the behavior of the ball to be nonlinear. The theoretical analysis has been carried out by assuming constant angular spacing between each ball.

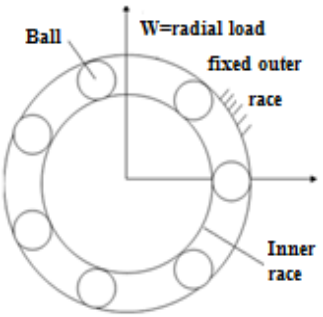

Fig. 1. A schematic diagram of ball bearing.

However, load deformation constant '*Kt'* between ball and ring is calculated based on contact geometry of ball bearing [18]. The typical dimensions of test bearing are as indicated in Table 1.

$$K_t=\left[\left(1/Kt_{ir}\right)^{-1.5}+\left(1/Kt_{or}\right)^{-1.5}\right]^{-1.5} \tag{3}$$

where $Kt_{ir}=3.12\times10^{7}\times\left(\varepsilon\rho_i\right)^{-0.5}\times\left(\delta_i*\right)^{-1.5}$ (4)

$$Kt_{or}=3.12\times10^{7}\times\left(\varepsilon\rho_o\right)^{-0.5}\times\left(\delta_o*\right)^{-1.5} \tag{5}$$

where $\delta i^{*}$and δo^{*} is dimensionless contact deformation based on curvature difference, $\in \rho i$ and $\in \rho o$ are curvature sum for bearing inner and outer race.

Table 1. Specification of ball bearing.

Property	**Value**
Make: Delux Bearings ;Bearing Number: DFM-85	
Ball mass (m_b)	0.0293 kg
Inner ring mass (m_{in})	0.18 kg
Outer ring mass (m_{out})	0.215 kg
Rotor mass(M)	3.0 kg
External diameter of bearing (d_o)	85 mm
Max. Dynamic load capacity (kg)	4635.9 kg
Max. Static load capacity (kg)	2518.6 kg
Bore diameter,(d_i)	30 mm
Diameter of ball (d_b)	17.463 mm
Number of balls (n_b)	7
Bearing Pitch Diameter (D_p)	57.5 mm
Radial Load (W)	1000 N
Defect Angle on Outer race (θ_d)	15degrees

3.1. **Defect model**

Local defects and waviness in the ball bearing are engendered mainly due to fatigue and error in manufacturing. Many researchers have analytically modelled vibrations generated in the ball bearing due to such type of defects. It has been concluded that majority of bearing fails due to fatigue [1]. Moreover, [19] it is observed that localized defects are frequently developed in the bearing raceway during its operation and

noticed that during running condition of bearing, entry and exit edge of local defect wears, which tends to spread size of the defect. But, when bearings are subjected to variable loading, such type of local defects tends to grow along the path of a point of contact between the ball and raceway, considered as extended raceway defect. In the present work, it is termed as a distributed type of defect. The present distributed kind of defect on the raceway has been characterized as an enlarged localized defect, whose arc length is not more than the spacing between two balls. It can also be categorized as defect smaller than the waviness. The surface defect has been described by simple sinusoidal function as shown in Fig. 2, noted by amplitude '*Ra'* and wavelength 'λ'. The amplitude defect at contact angle is given by:

$$w_{ampo} = R_a\left(nw_o \times \theta_o\right) \tag{6}$$

where, nw_o is the number of sinusoidal waves on the outer ring defect surface, which are assumed as '8' in current analysis and Ra, is the outer ring defect amplitude. Hence, the angular position of defect on outer race Θ_o is given by:

$$\theta_o = \left(\omega_c t\right) + \left(\theta_d \frac{\left(i-1\right)}{n_b}\right) \tag{7}$$

where 'ω_c' is the cage velocity, and $'\theta_d' = 15\,\pi/180$ is the defect angle of the outer ring. $i = 1,2,\ldots\ldots, n_b$; '$n_b$'=number of balls.

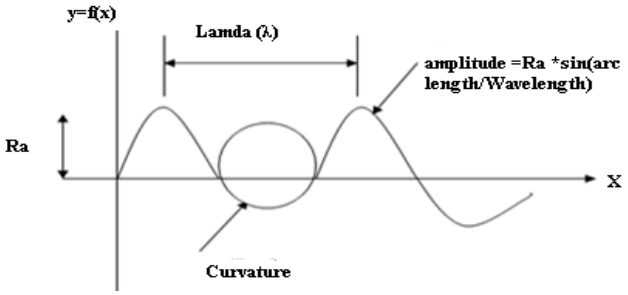

Fig. 2. Sinusoidal wave of outer ring defect.

3.2. **Equation of motion**

Dynamic analysis of ball bearing has been carried out by using Lagrange's equation of motion is given as follows:

$$\frac{d}{dt}\left(\frac{\partial E}{\partial \dot{x}}\right) - \left(\frac{\partial E}{\partial x}\right) + \left(\frac{\partial U}{\partial x}\right) = \left(f\right) \tag{8}$$

where '*E*' is kinetic energy, '*U* ' is potential energy, '*x*' is a vector of a generalized degree-of freedom coordinate and '*f*' is generalized excitation force vector. The energy developed by each bearing elements such as the ball, inner ring and outer ring has been derived separately. Figure 3 shows a model of bearing, whose kinetic energy is represented by the spring-mass system. The sum of kinetic energies of individual bearing elements is given as follows:

$$E = E_b + E_{ir} + E_{or} \tag{9}$$

The deformation of the ball with raceway contact produces the potential energy in the bearing system.

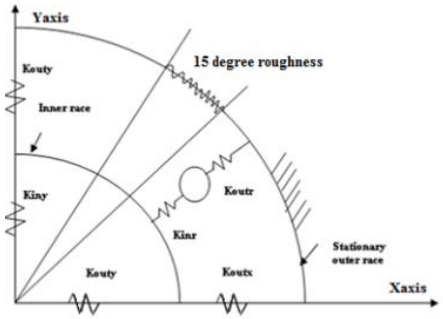

Fig. 3. Spring mass system of bearing.

The sum of potential energy generated by each bearing element is given as follows, where U_b, U_{or}, and U_{ir} are potential energies due to deformation of ball, inner ring and outer ring respectively.

$$U = U_b + U_{ir} + U_{or} \tag{10}$$

3.2.1. Inner ring analysis

Analysis of inner ring is carried out by assuming it as rigid body. Inner ring generates kinetic energy with reference to its mass center and has been computed in X and Y direction by using Eq. (11):

$$E_{ir} = \frac{1}{2} \times m_{in} \times \left(\dot{z}_{in} \times \dot{z}_{in} \right) + \frac{1}{2} \times I_{in} \times \omega_{in}^{\ 2} \tag{11}$$

where I_{in}, ω_{in} are the moment of inertia and inner ring velocity. z_{in} represent displacement of inner ring center with reference to outer ring center given by Eq. (12).

$$z_{in} = \left(x_{in} + x_{out} \right) i + \left(y_{in} + y_{out} \right) j \tag{12}$$

The potential energy produced due to deformation of inner ring with reference to outer ring center is given by Eq. (13).

$$U_{ir} = \frac{1}{2} Kt_{inx} \left(\dot{x}_{in} \right)^2 + \frac{1}{2} Kt_{iny} \left(\dot{y}_{in} \right)^2 \tag{13}$$

3.2.2. Outer ring analysis

Analysis of outer ring is carried out assuming it as rigid body and considered to be stationary. Therefore, the kinetic energy developed by the outer ring of bearing will be zero. Hence, E_{or}=0. Potential energy produced due to displacement of outer ring with reference to its center is given by Eq. (14):

$$U_{or} = m_{out} \times g \times y_{out} \tag{14}$$

3.2.3. Rolling element (Ball) analysis

The Kinetic energy of ball is described by three translational degrees of freedom $\dot{z_b}, v_{b,} \omega_b$ represented as ball velocity along its contact, center of gravity and its axis

respectively. The sum of kinetic energies developed by individual ball is given by Eq. (15):

$$E_b = \sum_{j=1}^{n_b} \frac{1}{2} m_b \dot{z}_b^{\,2} + \frac{1}{2} m_b v_b^{\,2} + \frac{1}{2} I_b \omega_b^{\,2} + \frac{1}{2} m_b \left(\dot{x}_{in}^2 + \dot{y}_{in}^2 \right) \tag{15}$$

The stiffness of ball due to nonlinear contact between ball and races develops potential energy in the bearing. The individual ball can store this energy is given by Eq. (16):

$$U_b = \int_0^{\delta} K_t \delta^3 d\delta = \frac{K_t \delta^4}{4} \tag{16}$$

where K_t and δ are the ball stiffness and ball deflection respectively. The contact stiffness between two deforming surfaces by assuming two surfaces made of steel are represented by Eq. (17).

$$\begin{aligned} Kt_{ir} &= Kt_{inx} \sqrt{\delta_{inr}} \\ Kt_{or} &= Kt_{outx} \sqrt{\delta_{outr}} \end{aligned} \tag{17}$$

where δ_{inr} is the contact deformation of ball with reference to inner ring and δ_{outr} is the contact deformation of ball with reference to outer ring. The potential energy generated by each ball considering defect on outer ring of bearing given by Eq. (18).

$$U_b = \frac{1}{2} Kt_{or} \left(z_b - w_{ampo} \right)^4 + \frac{1}{2} Kt_{ir} \left(z_b \right)^4 \tag{18}$$

Total potential and kinetic energies developed by all bearing elements are calculated by substituting the energies contributed by each element of ball bearing in Eqs. (9) and (10) respectively. The equation of motion of each rolling element of bearing can be obtained by differentiating it with respect to z_b, x_{ir}, y_{ir} and is given by Eq. (19).

$$m_b \ddot{z}_b + Kt_{or} \left(z_b - w_{ampo} \right)^3 + Kt_{ir} \left(z_b \right)^3 = 0 \tag{19}$$

Here, Kt_{ir}, Kt_{or} and w_{ampo} calculated from Eq. (19) and represents the excitation force of this equation. Positive sign in above equation signifies that if entity inside the bracket is positive, the balls are in load zone, which develops restoring force. Hence, equation of motion of bearing are represented by Eqs. (20) and (21).

$$\left(m_b + m_{in} \right) \ddot{x}_{in} + Kt_{inx} x_{in} = \left\langle f_x \right\rangle \tag{20}$$

$$\left(m_b + m_{in} \right) \ddot{y}_{in} + Kt_{iny} x_{in} = \left\langle f_y \right\rangle \tag{21}$$

Here, f_x and f_y represents the excitation force generated by outer ring along 'x' and 'y' directions. The equation of motion in 'x' direction is assumed to be the result of an imbalance force of the rotor, which is given by the expression.

$$f_x = m_{rotor} \times e \times \omega_{in}^{\,2} \times \sin\left(\omega_{in} \times t \right) \tag{22}$$

whereas, equation of motion in 'y' direction is assumed to be the result of radial load and imbalance force, is represented by Eq. (23):

$$f_y = W + [m_{rotor} \times e \times \omega_{in}^2 \times \sin\left(\omega_{in} \times t \right)] \tag{23}$$

where ω_{in} is the inner ring angular velocity and W is applied radial load.

4. Numerical Results

The vibration response predicted from the outer ring of the bearing and equation of motion described by each bearing element is represented by Eqs. (19), (20) and (21).The Runge Kutta technique was applied to solve these equations. The theoretical and experimental results at different speeds and defect sizes have been plotted, and comparison has been made. It has been observed that theoretical results obtained by Lagrangian approach are consistent with experimental results. In the present analysis time step is assumed to be $\Delta T = 10^{-3}$ seconds to have sufficient accuracy. At time $t = 0$, each rolling element initial displacement has considered being $z_1, z_2, z_3, z_4, z_5, z_6, z_7=10^{-3}$ mm along with the normal internal radial clearance. The deep groove ball bearing (DFM-85) of a single row with an extended distributed defect on its outer ring is considered in the analysis. Initially, the fault is assumed to be in contact with one of the balls and held at the center of the loaded region in line with the applied radial load. The numerical results are represented in acceleration amplitude. With the help of the MATLAB program, the acceleration amplitudes of bearing vibrations are evaluated for significant frequency components using Lagrangian method. The results revealed that there is a significant change in the amplitude of vibration with the change in defect size and speed.

4.1. Effect of speed

The vibration response of the bearing is measured by varying speed and its effect is analysed. The theoretical frequency domain responses are plotted as shown in Figs. 4 to 7, at 300, 600, 900 and 1200 rpm The arc length of raceway defect size, along the direction of rotation is taken as 15 degrees having a number of waves $nw_o = 8$. The depth of defect corresponds to the RMS amplitude of sinusoidal waves, is taken as $Ra = 10$ µm. The results are evaluated at 1000 N radial load.

The impulses are obtained at a frequency of 12.6, 24.54, 37.03, and 51.31 Hz. A significant rise in amplitude of vibration is observed with increase in speed. In this case, the acceleration amplitudes are found as 38.18 (0.03818 m/s^2), 473.1 (0.4731 m/s^2), 1484 (1.484 m/s^2), 2508 (2.508 m/s^2) mm/s^2 at respective range of speed. Hence, speed is major responsible parameter to increase vibration response of bearing.

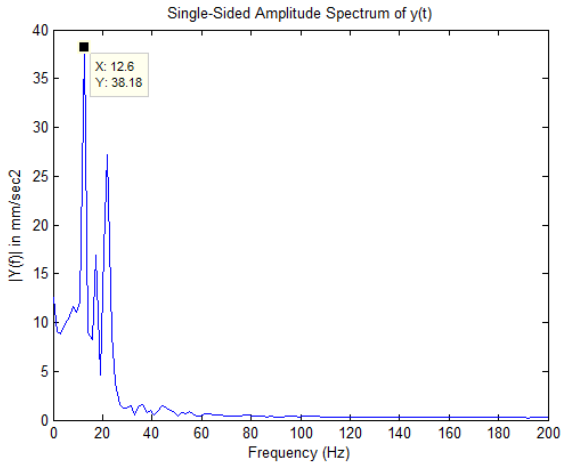

Fig. 4. Frequency spectrum of outer race defective bearing at 300 rpm.

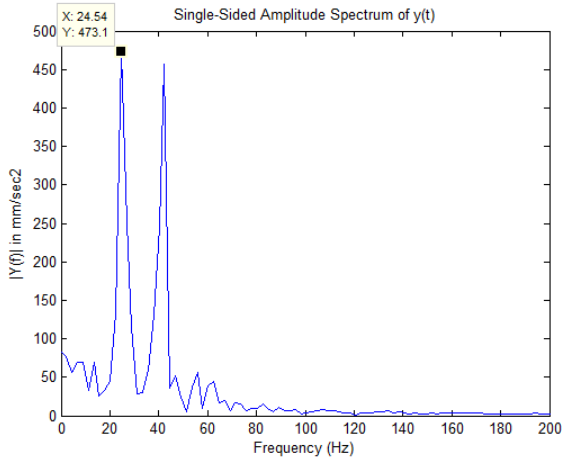

Fig. 5. Frequency spectrum of outer race defective bearing at 600 rpm.

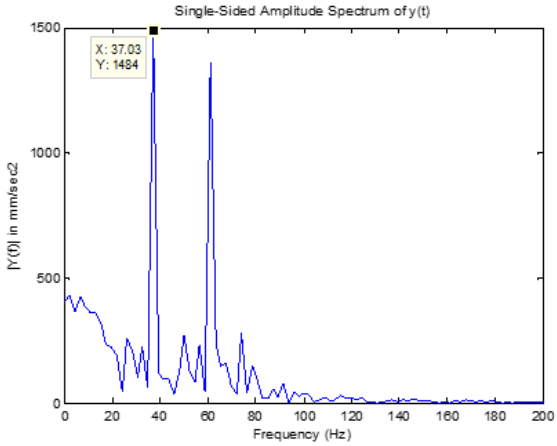

Fig. 6. Frequency spectrum of outer race defective bearing at 900 rpm.

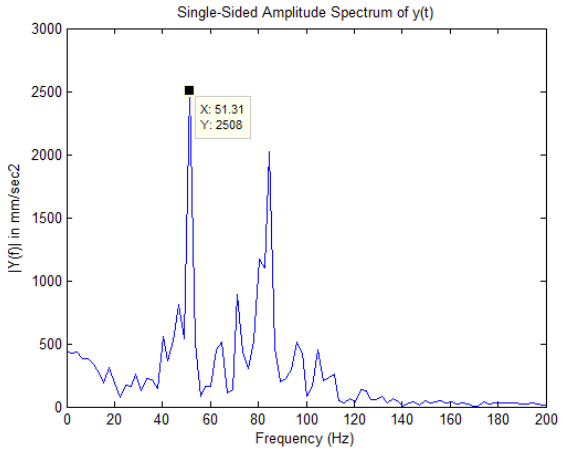

Fig. 7. Frequency spectrum of outer race defective bearing at 1200 rpm.

4.2. **Effect of defect size (Theoretical model)**

The vibration amplitude of acceleration is obtained by changing the size of outer race defect and the effect is measured on vibration response of bearing. All the observations were plotted under 1000 N radial load at 1200 rpm, whereas the amplitude of the defect was increased from Ra_1 (10 microns) to Ra_4 (40 microns). The frequency spectrum of bearing with outer race defect sizes of 20, 30 and 40 microns are as shown in Figs. 8 to 10. Peaks at the dominant frequency of 51.31 Hz are seen in model FFT plot. The amplitude of vibrations are observed as 2508 (2.508 m/s^2), 2754 (2.754 m/s^2), 4250 (4.25 m/s^2), 5925 (5.925 m/s^2) mm/s^2, at defect size of 10, 20, 30 and 40 microns respectively. It is observed that the frequency obtained from the theoretical model is close to experimentally obtained BPFO (49.13 Hz).

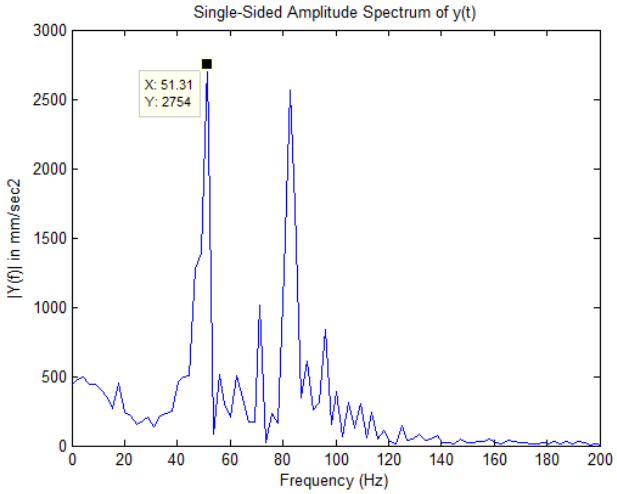

Fig. 8. Theoretical freq. spectrum with outer race defect size Ra_2.

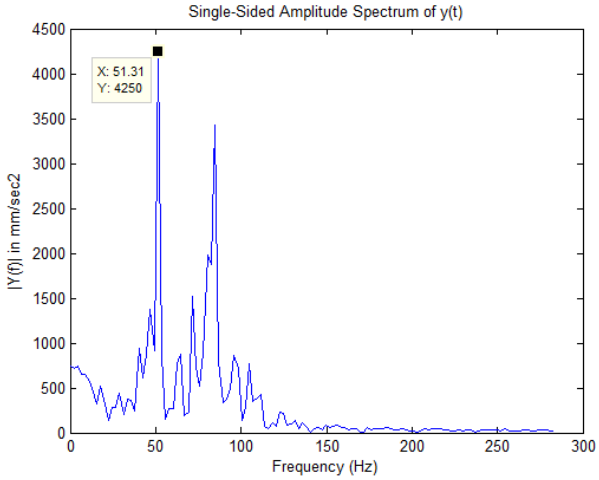

Fig. 9. Theoretical freq. spectrum with outer race defect size Ra_3.

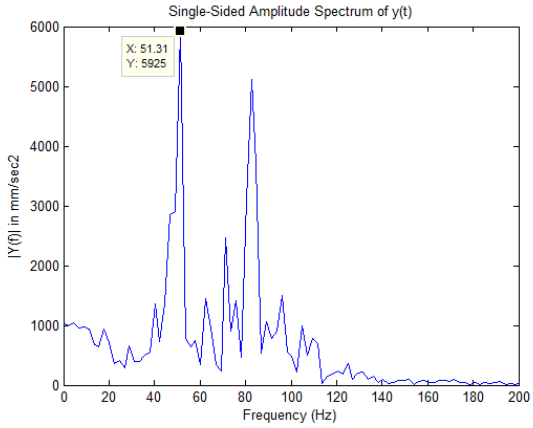

Fig. 10. Theoretical freq. spectrum with outer race defect size Ra_4.

Also the amplitude of acceleration with reference to this defect frequency has been increased with the change in the size of defect. These responses show that the size of defect is major influencing parameter to increase the vibration response of bearing.

5. Experimental Setup and Instrumentation

To investigate vibration characteristics obtained from faulty bearing and to monitor its condition the experimental test rig was designed. Figure 11 shows the experimental test rig. The results evaluated from theoretical model are compared with experimental results acquired from designed test rig. In the present experimental investigation, the extended distributed faults have been artificially introduced on outer ring of the bearing. The artificial defect is produced by electro-discharge machining as shown in Fig. 12. The special purpose bearings DFM- 85 are used as test bearing normally used in four wheeler engines. It was mounted in bearing housing on the shaft and loaded by turnbuckle in radial direction.

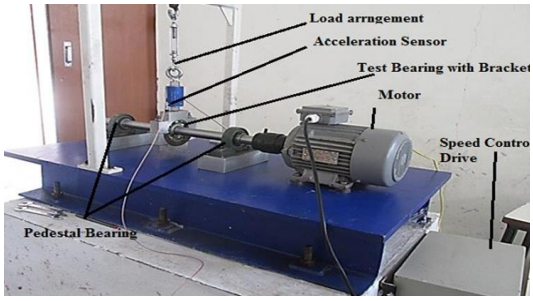

Fig. 11. Experimental test rig.

Fig. 12. Outer race defect.

The vibrations of bearing were recorded using piezoelectric accelerometer with the help of DEWOSOFT FFT analyzer. Vibration signals were acquired at different speeds up to 1200 rpm of the system for both normal and defective bearings. The signals are sampled at 5000 Hz with 2048 samples. During each separate

experimentation bearing was tested with defect size of Ra_1= 10 µm, Ra_2 = 20 µm Ra_3 = 30 µm and Ra_4 = 40 µm.

6. Experimental Results

The amplitudes of vibration were measured experimentally at various speed and defect sizes under specific load. The peak amplitudes are obtained at outer ring defect frequency of 11.90, 24.41, 36.62 and 49.13 Hz (BPFO), at speed 300, 600, 900 and 1200 rpm respectively. The results obtained through experimentation are in close agreement with the theoretical results. The sample experimental results under 1000 N radial load are represented in Figs. 13 to 16. The discussion in line with these findings is made in the next section.

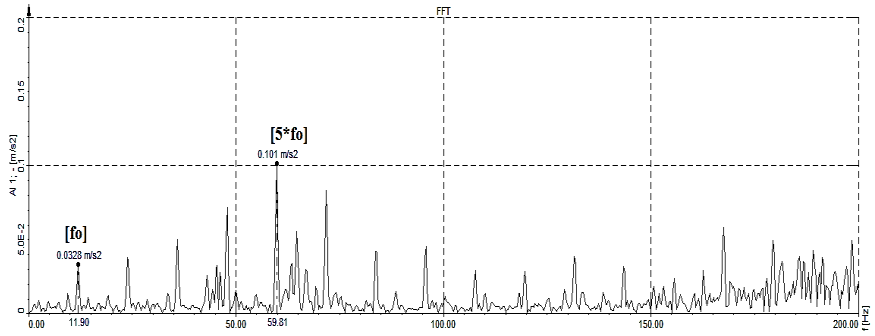

Fig. 13. Exp. Frequency spectrum of outer race defective bearing at 300 rpm.

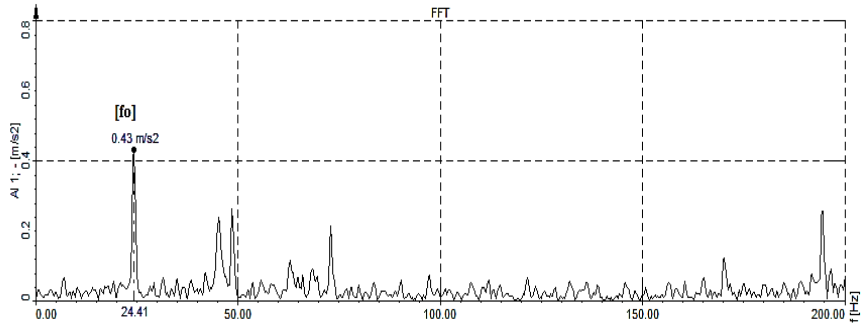

Fig. 14. Exp. Frequency spectrum of outer race defective bearing at 600 rpm.

Amplitudes of vibrations are measured at characteristic defect frequency and it has been observed that there is a significant rise in amplitudes of vibration with an increase in speed. In this case, the amplitudes of vibration for outer race defective bearing are 0.0328, 0.43, 1.39 and 2.38 m/s^2 at respective stated range of speed. For outer race defected bearing an average variation of 14 % in amplitudes of vibration is observed between theoretical and experimental values. However, at 300 rpm frequency spectra shows variation in frequency and amplitude throughout the signal. This may be because of variation in applied radial load and hence unbalancing, resonance generated due to the existence of defect in the ball bearing.

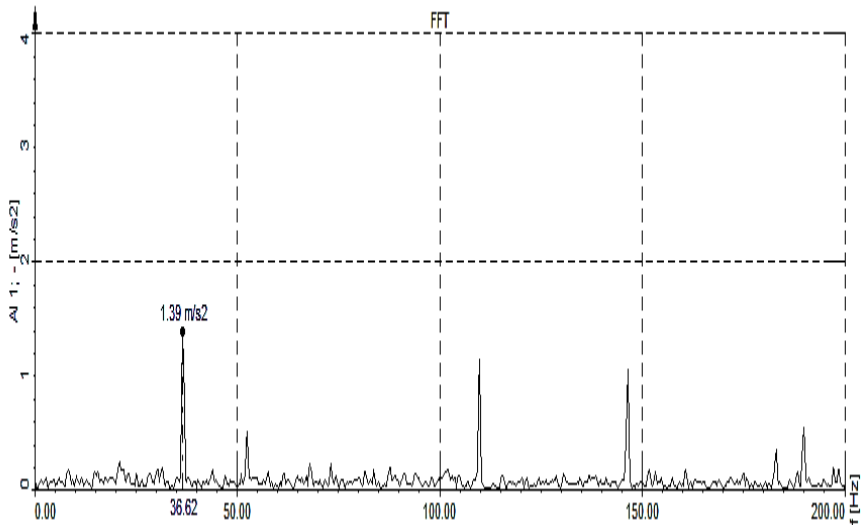

Fig. 15. Exp. Frequency spectrum of outer race defective bearing at 900 rpm.

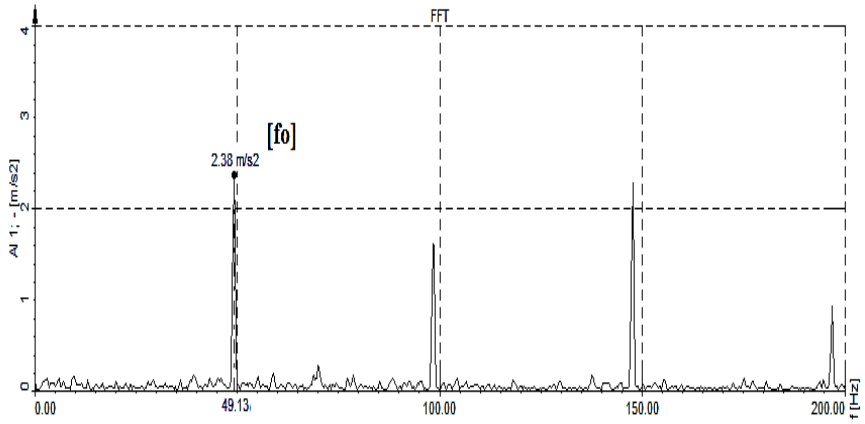

Fig. 16. Exp. Frequency spectrum of outer race defective bearing at 1200 rpm.

Effect of defect size (Experimental)

The effect of defect size on vibration response of outer race defected bearing is also measured experimentally. The observation were noted under same condition of load and speed i.e. at 1000 N radial load at 1200 rpm, whereas the amplitude of the defect was increased from Ra_1 (10 microns) to Ra_4 (40 microns). Peaks at the dominant frequency of 49.13 Hz are seen in frequency spectrum. The amplitude of vibrations are observed as 2.38, 2.6, 4.02 and 5.17 m/s^2 at defect size of 10, 20, 30 and 40 microns respectively. It is observed that the experimental defect frequency is close to frequency obtained from theoretical model (51.31 Hz). The same trend of effect of defect size on vibration response of bearing is observed as like theoretical analysis. Hence, it observed that the amplitude of acceleration with reference to this defect frequency has been increased with the change in the size of defect.

7. Discussion

The amplitude values of acceleration along with frequency of rotation have been standardized with respect to response amplitude acquired through experimentation at different outer ring characteristic frequencies are indicated in Table 2.The vibration responses are measured at different speed of at 300 to 1200 rpm. It is observed that the peak amplitude of acceleration has significant rise with increase in shaft speed. The amplitude values of acceleration obtained through theoretical model have been compared with experimental results. The amplitude variation of acceleration between the model responses is in fair agreement with experimental response. In addition to this, the percentage variation between the theoretical and experimental defect frequency is around 6 % whereas, the deviation in amplitude of acceleration is around 14% was observed between model and experimental response as indicated in Table 2. However, the responses obtained from both models are constrained to the components at defect frequency of outer ring and sidebands. Additional frequency components obtained from experimental analysis, particularly BPFO peaks with its multiple and frequency of shaft were not able to predict by present model. Moreover, the response of vibration amplitude obtained at 300 rpm may be because variation in applying radial load and hence deviation in frequency and vibration response is observed.

Table 2. Comparison of theoretical and experimental vibration response.

Speed in rpm	Theoretical Model Response		Experimental Response		% Error in Freq.	% Error in Amp.
	Freq. in Hz	Amp. m/s^2	Freq. in Hz	Amp. m/s^2		
300	12.60	0.03818	11.90	0.0328	5.56	14.09
600	24.54	0.4731	24.41	0.43	0.53	9.11
900	37.03	1.484	36.62	1.39	1.11	6.33
1200	51.31	2.508	49.13	2.38	4.25	5.10

8. Conclusions

The theoretical analysis has been carried out to obtain vibration response of ball bearing with single extended distributed type of defect on its outer ring. The response of derived model has been validated with experimental results under constant radial load. It was found that there is a significant rise in vibration amplitude with an increase in rotor speed. To analyse the effect of defect size and to predict the spectral components of vibration, sinusoidal wave is assumed to model the bearing defect. It can be concluded from the theoretical analysis that defect size has a major influence on vibration response of bearing. The model also predicts the peaks of the frequency spectrum, observed at BPFO, harmonics of BPFO and combination of cage frequency and shaft frequency. The frequency of components due to defects and vibration amplitude obtained from the theoretical analysis shows consistency in the results with results obtained from the experimental study. The vibration response of ball bearing with outer ring defect shows satisfactory results through experimentation. However, the effect of the entire rotor bearing system has not taken into account to predict the actual amplitude of vibration. Hence, analysis of bearing with an extended type of

distributed defect at normal speed, concludes that, speed and defect size are major influencing parameter to increase the vibration response of bearing even with low change in signal energy generated from the faults with variation in defect size.

Acknowledgements: The authors are thankful to the research and development department of DELUX bearings Pvt. Ltd. Sanaswadi, Pune (India) for making the availability of bearings and the test facility for the present investigation.

Nomenclatures

d_b	Ball diameter, mm
D_p	Pitch diameter, mm
E_b	Kinetic energy of ball, N-mm
E_{ir}	Kinetic energy of inner ring, N-mm
E_{or}	Kinetic energy of outer ring, N-mm
f	Excitation force in Lagrangian equation, N
fi	Outer and inner ring defect frequency, Hz
fo	Outer ring defect frequency, Hz
fs	Shaft frequency, Hz
$F\rho$	Curvature difference
Kt	Contact stiffness, N/mm
Kt_{inx}	Inner ring stiffness in x-direction, N/mm
Kt_{iny}	Inner ring stiffness in y-direction, N/mm
Kt_{ir}	Inner ring to ball contact stiffness, N/mm
Kt_{ir}	Inner ring to ball contact stiffness, N/mm
Kt_{or}	Outer ring to ball contact stiffness, N/mm
m_b	Mass of ball(gram
m_{in}	Inner ring mass, gram
U_b	Potential energy of ball, N-mm
U_{or}	potential energy of outer ring, N-mm
W	Radial load, N
w_{ampo}	Amplitude of outer ring defect, micron
x_{in},, y_{in}	Inner ring center with respect to x and y reference
x_{out}, y_{out}	Outer ring center with respect to x and y reference
z_j	Ball deflection , mm

Greek Symbols

δ^*	Dimensionless parameter
δ_{inr}	Deflection of ball along inner ring, mm
δ_{outr}	Deflection of ball along outer ring, mm
θ_d	Defect angle, degree
θ_o	Angular position of defect, degree
λ	wavelength of surface defect
ω_c	Angular velocity of cage, rad/s
ω_{in}	Angular velocity of inner ring rad/s

Abbreviations

BPFO	Ball Pass Outer race frequency
BPFI	Ball Pass Inner race frequency

References

1. Sadeghi, F.; Jalalahmadi, B.; Slack, T.S.; Raje, N.; and Arakere, N.K. (2009). A review of rolling contact fatigue. *Journal of Tribology*, 131(4), 041403-041403-15.
2. Maharjan, N.; Zhou, W.; and Zhou, Y. (2016). Micro-structural study of bearing material failure due to rolling contact fatigue in wind turbine gearbox. *Proceedings of 6th International Symposium on Current Research in Hydraulic Turbines*, Paper no. CRHT2016-12.
3. Howard, I. (1994). A review of rolling element vibration: detection, diagnosis and prognosis. *Technical report DSTO- RR*-0013, Defence science and Technology Organization, Australia.
4. Tandon, N.; and Choudhury, A. (1999). A review of vibration and acoustic measurement methods for the detection of defects in rolling element bearings. *Tribology International*, 32(8), 469-480.
5. Utpat, A.; Ingle, R.B.; and Nandgaonkar, M. (2011). Response of various vibration parameters to the condition monitoring of ball bearing used in centrifugal pumps. *Noise and Vibration Worldwide*, 42(6), 34-40.
6. McFadden, P.D.; and Smith, J.D. (1985). Model for the Vibration produced by a Multiple Point Defect in Rolling Element Bearing. *Journal of Sound and Vibration*, 98(2), 263-273.
7. Choudhary, A.; and Tandon, N. (2006).Vibration response rolling element bearings in a rotor bearing system to a local defect under radial load. *Journal of Tribology*, 128(2), 252-261.
8. Patil, M.S.; Mathew, J.; Rajendrakumar, P.K.; and Desai, S. (2010). A theoretical model to predict the effect of localized defect on vibrations associated with ball bearing. *International Journal of Mechanical Science*, 52(9), 1193-1201.
9. Patel, V.N.; Tandon, N.; and Pandey, R.K. (2010). A dynamic model for vibration studies of deep groove ball bearings considering single and multiple defects in rings. *Journal of Tribology*, 132(4), 041101-041101-10.
10. Sopanan, J.; and Mikola, A. (2003). Dynamic model of a deep groove ball bearing including localized and distributed defects. *Part 1: Theory, Proceeding of the Institution of Mechanical Engineers, Part K: Journal of Multi-Body Dynamics*, 217, 210-211.
11. Meyer, L.D.; Ahlgren, F.F.; and Weichbrodt, B. (1980). An analytical model for ball bearing vibration to predict vibration response with distributed defects. *Journal of Mechanical Design*, 102(2), 205-210.
12. Tandon, N.; and Choudhury, A. (2000). A theoretical model to predict the vibration response of rolling bearings in a rotor bearing system to distributed defects under radial load. *Journal of Tribology*, 120(3), 214-220.
13. Tiwari, M.; Gupta, K.; and Prakash, O. (2000). Effect of radial internal clearance of a ball bearing on the dynamics of a balanced horizontal rotor. *Journal of sound and vibration*, 238(5), 723-756.
14. Harsha, S.P.; and Kankar, P.K. (2004). Stability analysis of a rotor bearing system due to surface waviness and number of balls. *International Journal of Mechanical Sciences*, 46(7), 1057-1081.

15. Petersen, D.; Howard, C.; Sawalhi, N.; Ahmadi, A.M.; and Singh, S. (2014). Analysis of bearing stiffness variations, contact forces and vibrations in radially loaded double row ball bearings with raceway defects. *Mechanical Systems and Signal Processing*, 50-51, 139-160.
16. Behzad, M.; Bastami, A.R.; and Mba, D. (2011). A new model for estimating vibrations generated in the defective rolling element bearings. *Journal of Vibration and Acoustics*, 133(4), 041011.
17. Sawalhi, N.; and Randall, R.B. (2008). Simulating gear and bearing interactions in the presence of faults: Part II: Simulation of the vibrations produced by extended bearing faults. *Mechanical Systems and Signal Processing*, 22(8), 1952-1966.
18. Harris, T.A.; and Kotzalas, M.N. (2007). *Essential concepts of bearing technology* (6th ed.). New York: John Wiley and sons Inc.
19. Singh, S.; Howard, C.Q.; and Hansen, C.H. (2015). An extensive review of vibration modeling of rolling element bearings with localized & extended defects. *Journal of Sound and Vibration*, 357, 300-330.